11th International Symposium on Magnetic Bearings
August 26-29, Nara, Japan

A Controller Design to Suppress the Interference Force of the Propulsion Equipment Acting on the Suspension System in a Magnetically Levitated Train System

Jun-Ho Lee
Korea Railroad Research Institute, 360-1 Woulam-Dong, Uiwang-City Kyonggi-Do, Korea 437-757, tel: +82-31-460-5040, fax: +82-31-460-5449, E-mail: jhlee77@krri.re.kr

ABSTRACT

In this paper we deal with a design of integral sliding mode controller to reject the disturbance force acting on the suspension system in a magnetically levitated system which is propelled by the linear induction motor. The control scheme consists of an integral compensator which is designed to achieve zero steady-state error under step disturbances, and a sliding mode controller which is designed for enhancing robustness under plant uncertainties. A proper continuous design signal is introduced to overcome the chattering problem. The disturbance force produced by the linear induction motor is formularized by using a curve fitting method. Computer simulations show the effectiveness of the designed integral sliding mode controller to reject the disturbance force in comparison with a simple sliding mode controller that does not include the integral compensator.

INTRODUCTION

One of the ways that maintain non-contact states between two materials is to employ a magnetic suspension technology [1]. This system is commonly known as Magnetically Levitated system (*Maglev*) which has been used in the vehicle levitation system and magnetic bearing system developed in the University of Virginia, U.S.A. in 1937 for the first time. There are various applications employing the magnetic levitation configuration as a key technology, such as the magnetically levitated train system[1][6], the high speed turbo compressors[2][4], the flywheel energy storage system[3], and the artificial heart pump [5].

The magnetically levitated train system can be divided into two parts based on the levitation method: one is a repulsive type using super conductors. A disadvantage of this type of suspension system is needed for operation below the critical speed when the suspended object is stationary. The other type is using ferromagnetic or permanent magnet. This type of electromagnetic suspension system (EMS system) has one significant advantage in that it provides attraction force at zero speed, but such system is inherently unstable. In order to overcome the inherent instability an active controller plays a very important role in the electromagnet suspension system to make the stable suspension and to maintain the suspended object within the nominal air gap.

Especially in the magnetically levitated train system external disturbance force acting on the controller may cause the malfunction of the suspension system. If a *Maglev* train is propelled by the linear induction motor the suspension controller of the *Maglev* train should have a capability to reject the normal force produced from the linear induction motor. The reason is because the normal force of the linear induction motor acts as the disturbance force on the suspension controller.

In this paper we deal with a design procedure for the integral sliding mode controller to reject the disturbance force acting on the suspension controller[4][5]. First we present a simple mathematical model for the *Maglev* train and then introduce the integral sliding mode controller. Second a mathematical formula for the normal force of the linear induction motor is derived by the curve fitting of the experimental data. Finally we show the effectiveness of the integral sliding mode controller to reject the disturbance force by the dynamic simulation in comparison with the simulation results for the sliding mode controller that does not include the integral compensator.

MATHEMATICAL MODEL

Fig.1 shows a simple schematic diagram for EMS system which has the electromagnets as the suspension actuators, linear induction motor and reaction plate for the vehicle propulsion. As

shown in Fig. 1, the passenger vehicle and the bogie can be levitated by the electromagnets attraction force. Once the bogie is levitated, the propulsion system (linear induction motor and reaction plate) is activated to move the passenger vehicle.

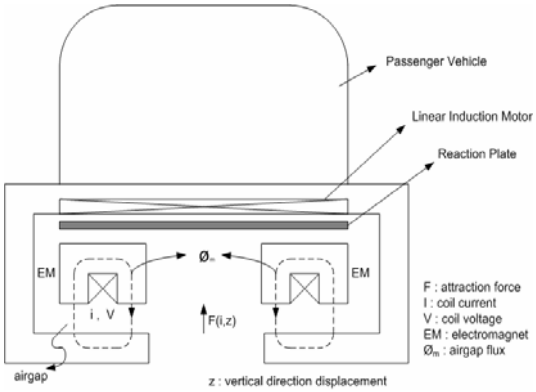

Fig. 1. Schematic diagram for EMS system

Fig. 2 is the simplified equivalent model of the suspension system shown in Fig. 1. The mathematical model of this system is divided into two parts: One is the plant (mechanical) dynamics and the other is the actuator dynamics.

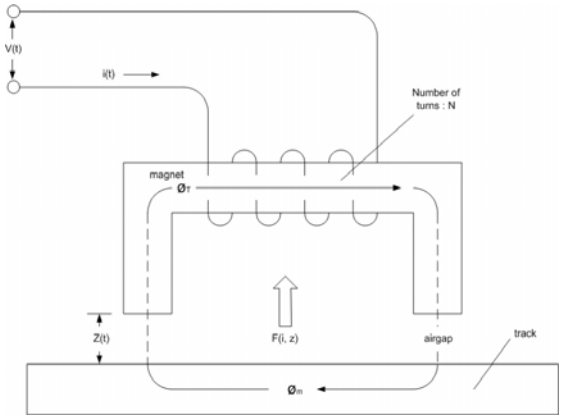

Fig. 2. Simplified schematic diagram

The plant dynamics is

$$m\ddot{z} = F(i,z) - mg - f_d \tag{1}$$

where m is the total mass of the controlled object, g is the gravitational acceleration, and f_d is the external disturbance force acting on the controlled object. In eq. (1), $F(i,z)$ is the electromagnets attraction force which is proportional to the current deviation and inversely proportional to the air gap deviation, expressed such as:

$$F(i,z) = \frac{B^2 A}{\mu_0} = \frac{\mu_0 N^2 A}{4}\left(\frac{i(t)}{z(t)}\right)^2 \tag{2}$$

where B is the flux density of the magnetic core material, A is the cross sectional area of the pole face of the electromagnet, μ_0 is the permeability in the air space, and N is the number of turns. Since eq. (2) has high nonlinearity it is necessary that the linear approximation should be carried out for the analysis of eq. (2) with respect to the nominal point (i_0, z_0). The Taylor Series Expansion is usually employed. From the Taylor Series Expansion the eq. (2) becomes

$$F(i,z) = k_i i(t) - k_z(t) \tag{3}$$

where $k_i = \frac{\mu_0 N^2 A i_0}{2z_0^2}$ and $k_z = \frac{\mu_0 N^2 A i_0^2}{2z_0^3}$.

The actuator dynamics is

$$\begin{aligned} v(t) &= Ri(t) + \frac{d}{dt}\left[L(i,z)i(t)\right] \\ &= Ri(t) + \frac{\mu_0 N^2 A}{2z(t)}\frac{d}{dt}i(t) - \frac{\mu_0 N^2 A i_0}{2z(t)^2}\frac{d}{dt}z(t) \end{aligned} \tag{4}$$

where v is the coil voltage, R is the coil resistance, and $L(i,z)$ is the magnet inductance which is the function of the air gap displacement such as $L(i,z) = \frac{\mu_0 N^2 A}{2z(t)}$. There is a variation of the inductance with respect to the air gap deviation in the second term of Eq. (4), and that the third term denotes a voltage which varies with changes in the air gap $z(t)$ and its rate of change similar to back EMF voltage.

By using equations (1), (3) and (4) the state space equations are written in the vector matrix form:

$$\begin{bmatrix} \dot{z} \\ \ddot{z} \\ \dot{i} \end{bmatrix} = \begin{bmatrix} 0 & 1 & 0 \\ \frac{-k_z}{m} & 0 & \frac{k_i}{m} \\ 0 & \frac{k_z}{k_i} & \frac{-R}{L} \end{bmatrix} \begin{bmatrix} z \\ \dot{z} \\ i \end{bmatrix} + \begin{bmatrix} 0 \\ 0 \\ \frac{1}{L} \end{bmatrix} v + \begin{bmatrix} 0 \\ \frac{1}{m} \\ 0 \end{bmatrix} f_d \tag{5}$$

where f_d is the normal force of the linear induction motor which acts. Eq. (5) can be simply expressed as

$$\dot{x} = Ax + Bu + Bf_d \tag{6}$$

Where

$$A=\begin{bmatrix} 0 & 1 & 0 \\ \frac{-k_z}{m} & 0 & \frac{k_i}{m} \\ 0 & \frac{k_z}{k_i} & \frac{-R}{L} \end{bmatrix}, B=\begin{bmatrix} 0 \\ 0 \\ \frac{1}{L} \end{bmatrix}, \quad E=\begin{bmatrix} 0 \\ \frac{1}{m} \\ 0 \end{bmatrix}$$

INTEGRAL SLIDING MODE CONTROLLER

To enhance the disturbance rejection capabilty, we introduce an integrator as a state variable into (5). The integrator output z_i is expressed as the difference between the integrated reference position r and integrated position z written as:

$$z_i = \int (r - z)dt \tag{7}$$

where r is zero for a nominal design. The block diagram of the proposed control system is shown in Fig. 3.

In order to synthesis the integral sliding mode controller we write the state variables as, $x=\begin{bmatrix} z_i & z & \dot{z} & i' \end{bmatrix}$ and get the following state space matrices.

$$A=\begin{bmatrix} 0 & -1 & 0 & 0 \\ 0 & 0 & 1 & 0 \\ 0 & \frac{-k_z}{m} & 0 & \frac{k_i}{m} \\ 0 & 0 & \frac{k_z}{k_i} & \frac{-R}{L} \end{bmatrix}, \quad B=\begin{bmatrix} 0 \\ 0 \\ 0 \\ \frac{1}{L} \end{bmatrix}, \quad E=\begin{bmatrix} 0 \\ 0 \\ \frac{1}{m} \\ 0 \end{bmatrix} \tag{8}$$

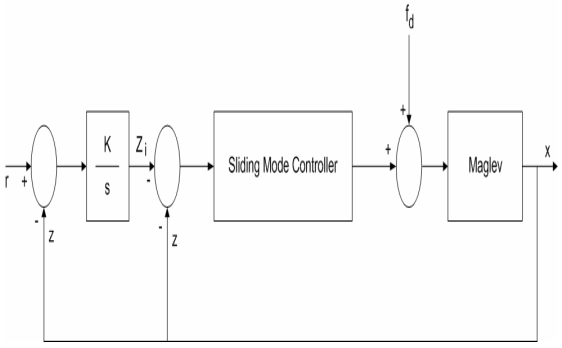

Fig. 3. Block diagram of an integral sliding mode controller for Maglev

Eq. (8) is decomposed as:

$$\begin{bmatrix} \dot{x}_1 \\ \dot{x}_2 \end{bmatrix} = \begin{bmatrix} A_{11} & A_{12} \\ A_{21} & A_{22} \end{bmatrix} \begin{bmatrix} x_1 \\ x_2 \end{bmatrix} + \begin{bmatrix} B_1 \\ B_2 \end{bmatrix} u \tag{9}$$

where

$$x_1=\begin{bmatrix} z_i \\ z \\ \dot{z} \end{bmatrix}, \; x_2 = i',$$

$$A_{11}=\begin{bmatrix} 0 & -1 & 0 \\ 0 & 0 & 1 \\ 0 & \frac{-k_z}{m} & 0 \end{bmatrix}, \; A_{12}=\begin{bmatrix} 0 \\ 0 \\ \frac{k_i}{m} \end{bmatrix},$$

$$A_{21}=\begin{bmatrix} 0 & 0 & \frac{k_z}{k_i} \end{bmatrix}, \; A_{22}=\frac{-R}{L}$$

$$B_1=\begin{bmatrix} 0 \\ 0 \\ 0 \end{bmatrix}, \; B_2=\frac{1}{L}, \; u=v \tag{10}$$

Let the switching surface be defined as $\sigma = Sx$ where

$$\sigma=\begin{bmatrix} S_1 & S_2 \end{bmatrix}\begin{bmatrix} x_1 \\ x_2 \end{bmatrix}, \; S_1 \in R^{1\times 3}, \; S_2 = R \tag{11}$$

If the system dynamics is an ideal sliding surface we have $\sigma = Sx = 0$. Using this property we can determine the equivalent system and associated linear control input. $\sigma = 0$ yields

$$x_2 = -\frac{S_1}{S_2}x_1 \tag{12}$$

Substituting (12) into (9) yields the equivalent system

$$\dot{x}_1 = (A_{11} - A_{12}S_2^{-1}S_1)x_1 \tag{13}$$

Defining $k = S_2^{-1}S_1$, we write (13) as

$$\dot{x}_1 = (A_{11} - A_{12}k)x_1 \tag{14}$$

The location of poles of the resulting system are obtained by selecting k and S_2 as the switching function becomes $\sigma = Sx$, $S=\begin{bmatrix} S_1 & S_2 \end{bmatrix}=\begin{bmatrix} S_2k & S_2 \end{bmatrix}=S_2\begin{bmatrix} k & 1 \end{bmatrix}$. Since (A_{11}, A_{12}) is controllable, a placement method is employed to select the gain k in (14). The sliding mode control inputs are separated into the linear and nonlinear components as $u = u_l + u_{nl}$.

The linear input u_l can be selected by the following equations:

$$\dot{x} = Ax + Bu \tag{15}$$

$$\dot{\sigma} = S\dot{x} = 0 \tag{16}$$

From eq. (15) and (16) we get the equivalent linear control input as :

$$u_l = -(SB)^{-1} SAx = -F_l x \tag{17}$$

The sliding mode reaching condition given by $\sigma\dot{\sigma} < 0$, brings the system dynamics to the sliding surface $\sigma = 0$. Choose the nonlinear control as $u_{nl} = -(SB)^{-1}\rho\,\mathrm{sgn}(\sigma)$ where $\rho > 0$ Then, it follows that

$$\begin{aligned}\sigma\dot{\sigma} &= \sigma S(Ax + Bu) \\ &= \sigma SAx - \sigma SB\left[(SB)^{-1} SAx + (SB)^{-1}\rho\,\mathrm{sgn}(\sigma)\right] \\ &= -\rho\sigma\,\mathrm{sgn}(\sigma)\end{aligned} \tag{18}$$

The control input can then be written as

$$u = -(SB)^{-1}\left[SAx + \rho\,\mathrm{sgn}(\sigma)\right] \tag{19}$$

In practice a discontinuous control component as $\mathrm{sgn}(\sigma)$ is undesirable because it may cause a chattering problem. The practical control effort is to ensure a neighborhood of $\sigma = 0$ is reached and maintained. A common choice of a practical nonlinear control input is

$$u_{nl} = -\rho\frac{\sigma}{|\sigma| + \delta} \tag{20}$$

where δ is the boundary layer which is selected to reduce the chattering problem and ρ is a design parameter.

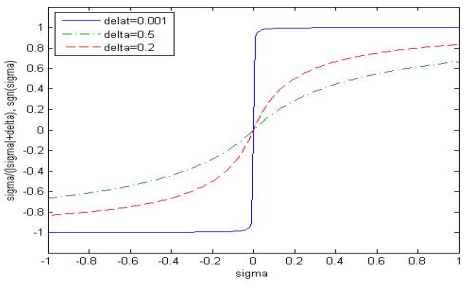

Fig. 4. Smooth approximation of the sgn function

Fig. 4 shows the relation between the discontinuous sgn function and continuous function. In this figure we can see that the slope of the continuous function depends upon δ . Fig. 5 shows the block diagram of the designed sliding mode controller connected to the integral compensator.

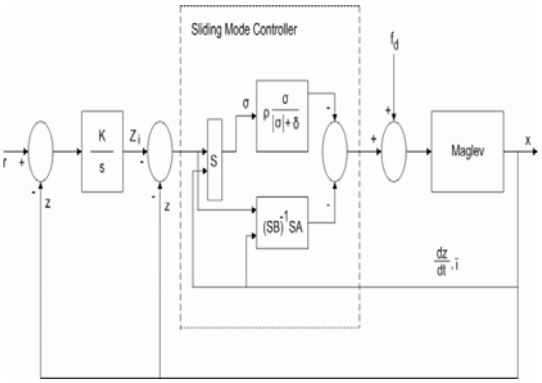

Fig. 5 Block diagram of integral sliding mode control implementation

CURVE FITTING FOR THE NORMAL FORCE

In this paper linear induction motor is employed as a propulsion system. The simple configuration is shown in Fig. 1. The linear induction motor is composed of primary coil and reaction plate as secondary. The thrust force and the normal force are dependant upon the relative displacement of the primary and the secondary [6]. The relative motion between the rotor and the stator can be expressed by introducing slip such as:

$$s = \frac{n_{slip}}{n_{sync}} \times 100\% \tag{21}$$

and

$$s = \frac{n_{sync} - n_m}{n_{sync}} \tag{22}$$

where s is the slip, n_{slip} is the slip speed of the motor, n_{sync} is the synchronized rotor speed, and n_m is the mechanical rotor speed. If the end effect is ignored the force property of the linear induction motor is dependant on the slip frequency which is defined as the difference in speed between the synchronized rotor speed and the mechanical rotor speed as:

$$n_{slip} = n_{sync} - n_m \tag{23}$$

(22) and (23) yield

$$n_m = (1-s)n_{sync} \tag{24}$$

Eq. (24) shows that if the mechanical speed of the rotor is equal to the synchronized rotor speed, $n_m = n_{sync}$ and $s = 0$ are satisfied, on the other hand if the mechanical rotor speed is zero, $n_m = 0$ and $s = 1$ are satisfied.

Fig. 6 shows the relation between force and slip. As shown in the figure as the slip increases the mechanical speed goes down. Fig. 7 shows the relation between the mechanical speed and the force produced by the linear induction motor. When the mechanical rotor speed is low (slip is close to one) the flux density is increased and the normal force acts as the attractive force in the linear motor which acts as the external disturbance force against the suspension system. On the other hand, when rotor speed goes up (slip is close to zero) the flux density is decreased and the normal force acts as the repulsive force in the linear motor which causes decrease of the suspension control current. Therefore the normal force is dependant upon the mechanical rotor speed and it is necessary to reduce the attractive force of the linear induction motor acting on the suspension system as the external disturbance force by the slip frequency control. For the simulation of the Fig. 7 we used the force data from Ref [6]. Fig. 8 shows the estimated normal force by using the curve fitting method. Eq. (25) represents the approximated formula which expresses the normal force.

$$F_n = p_1 v_m^2 + p_2 v_m + p_3 \tag{25}$$

where F_n is the normal force, p ($p_1 = -0.0109$, $p_2 = 13.0127$, $p_3 = -705.3725$) is the coefficient for the approximation, and v_m is the mechanical velocity.

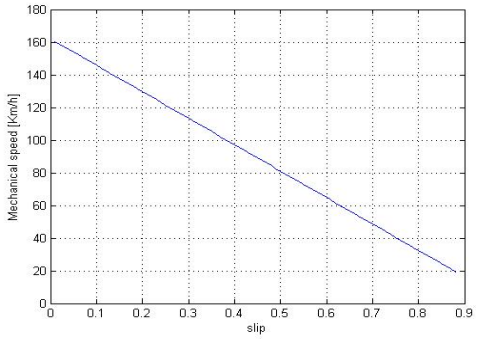

Fig.6 Slip and mechanical speed

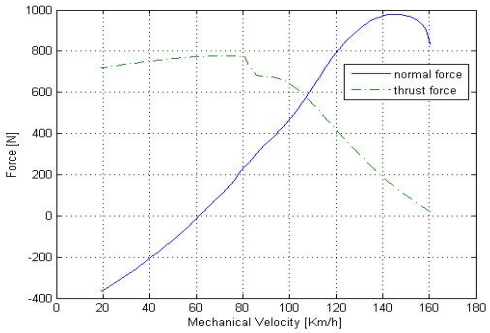

Fig. 7 Relation between the mechanical velocity and force

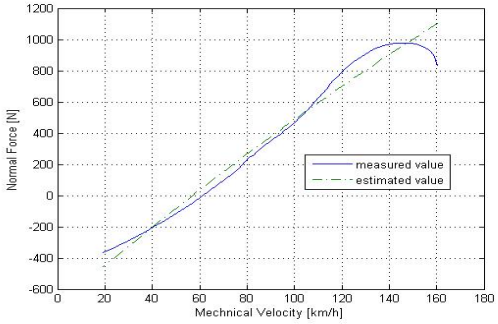

Fig. 8 Estimatied force

Eq. (25) and the Fig. 8 show the attractive force is maximum when v_m is close to zero. This analysis means that the suspension controller is affected by the 500[N] attractive normal force of the linear induction motor which acts as the external disturbance force at low speed and the suspension controller should has the capability to suppress the external disturbance force.

SIMULATIONS

Table 1. shows the parameters for the EMS type suspension system. The attractive force which acts on the suspension system as the external disturbance force is produced at low speed range, that is from 0[km/h] to 40[km/h]. The integral

sliding mode controller should be designed to reject the external disturbance force which is produced at very low speed.

Table 1. Parameters for suspension system

Parameters	Values
Turns	280[N]
Coil resistance	0.16[Ω]
Steady current	35[A]
Pole face area	4273×10^{-6} [m^2]
Nominal gap	10×10^{-3} [m]
Coil inductance	0.02[H]
Vehicle mass	500[Kg]

In this paper we employ a dynamic simulation model that the disturbance force acts on the integral sliding mode controller dynamically. The dynamic simulation model makes it possible that the effect of the normal force of the linear induction motor on the controller can be observed in the overall mechanical rotor speed range. In order to show the effectiveness of the integral sliding mode controller we make the comparison with the simulation results provided by the sliding mode controller that does not include integral compensator.

For the integral sliding mode controller we set the following controller parameters.

$$k = 10^5 \times [0.0161 \quad 0.006 \quad 1.375]$$

$$\rho = 50\,, \quad \delta = 0.4$$

Fig. 9 represents the gap deviation when the integral sliding mode controller is employed. To apply the disturbance force to the suspension system eq. (25) is used with the change of the mechanical speed v_m from 0[km/h] to 160[km/h]. Since eq. (25) provides the normal force as a function of the mechanical speed, it is possible to observe the effect of the normal force on the controller in the overall speed range. As shown in Fig. 9 *Maglev* vehicle is successfully suspended from the initial position (15×10^{-3} [m]) even if the normal force of the linear induction motor acts on the suspension system as the external disturbance force, and the gap deviation is maintained inside the nominal gap. Fig. 10 shows the rescaled of Fig. 9 to observe the low speed range.

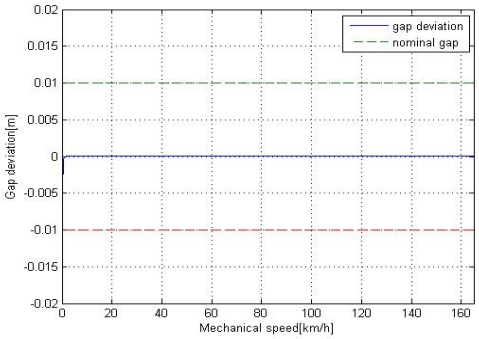

Fig. 9 Gap deviation : integral sliding mode controller

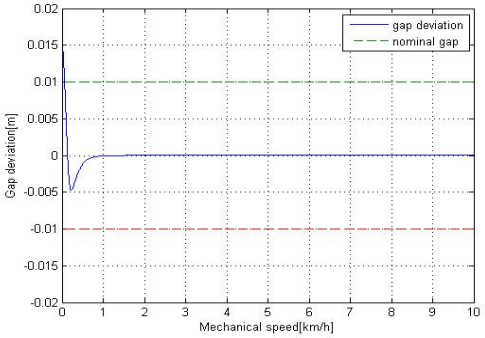

Fig. 10 Gap deviation (rescaled) : integral sliding mode controller

Fig. 11 is the simulation results when the sliding mode controller without integral compensator is employed. The same equation with the case of Fig. 9 is used to apply external disturbance force to the suspension system for making reasonable comparison. As shown in the figure the *Maglev* vehicle is not suspended and the gap deviation diverges from the nominal gap due to the external disturbance force produced by the linear induction motor. This means that integral compensator is very robust against the step type disturbance force as shown in Fig. 9 and Fig. 10.

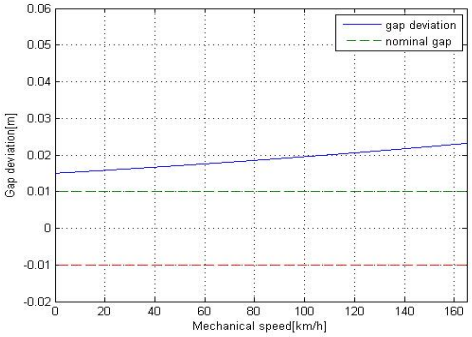

Fig. 11 Gap deviation : sliding mode controller without integral compensator

CONCLUSIONS

In this paper we dealt with the external disturbance force rejection property of the integral sliding mode controller in the magnetically levitated train system with the linear induction motor for propulsion system. The external disturbance force produced from the linear induction motor at low speed was applied to the suspension system with integral sliding mode controller and the suspension system with sliding mode controller without integral compensator to make the comparison of the simulation results.
First we showed the fundamental mathematical model of the magnetically levitated train, and then presented the synthesis of the integral sliding mode controller. For the normal force analysis of the linear induction motor we employed the curve fitting method. Finally the effective method of the integral sliding mode controller to suppress the external disturbance force was suggested and shown by the dynamic simulations.

References

[1] Edited by The Magnetically Levitation Technical Committee of The Institute of Electrical Engineers of Japan, ``Magnetic Suspension Technology: Magnetic Levitation System and Magnetic Bearings", *CORONA PUBLISHING CO, 1993*.

[2] Kenzo Nonami, Qi-fu Fan, Hirochika Ueyama, ``Unbalance Vibration Control of Magnetic Bearing Systems Using Adaptive Algorithm with Disturbance Frequency Estimation", *6th ISMB, August 5-7, 1998.*

[3] Jun-Ho Lee, Min-Soo Kang, Young-Woon Chung, Jung-Suk Lee, Key-Seo Lee, "Displacement-Sensorless Control of Magnetic Bearing System Using Current and Magnetic Flux Feedback", *The Transactions of the Korea Institute of Electrical Engineers D, Vol. 49D, No. 7, pp. 339-345, July, 2000.*

[4] Y. Fang, M. Feemster, D. Dawson, "Nonlinear Disturbance Rejection for Magnetic Levitation Systems", *Proceedings of the 2003 IEEE International Symposium on Intelligent Control, Huston, Texas, October 5-8, 2003*

[5] Jun-Ho Lee, P. E. Allaire, G. Tao, J. A. Decker, X. Zhang, "Experimental Study of Sliding Mode Control for a Benchmark Magnetic Bearing System and Artificial Heart Pump Suspension", *IEEE Transactions on Control System Technology, Vol. 11, No. 1, pp. 128-138, January, 2003.*

[6] Hyun-Gap Jeong, "Development of Maglev System for Urban Transit Application" *Korea Institute of Machinery & Materials Final Report, May, 1995*